AIP | Journal of Applied Physics

Boundary scattering effects during electron thermalization in nanoporous gold

Patrick E. Hopkins, Justin R. Serrano, Leslie M. Phinney, Hongqi Li, and Amit Misra

Citation: J. Appl. Phys. **109**, 013524 (2011); doi: 10.1063/1.3530866
View online: http://dx.doi.org/10.1063/1.3530866
View Table of Contents: http://jap.aip.org/resource/1/JAPIAU/v109/i1
Published by the American Institute of Physics.

Boundary scattering effects during electron thermalization in nanoporous gold

Patrick E. Hopkins,[1,a)] Justin R. Serrano,[1] Leslie M. Phinney,[1] Hongqi Li,[2] and Amit Misra[2]
[1]*Sandia National Laboratories, Albuquerque, New Mexico 87185, USA*
[2]*Los Alamos National Laboratories, Los Alamos, New Mexico 87545, USA*

(Received 17 September 2010; accepted 23 November 2010; published online 13 January 2011)

We study the electron relaxation processes in nanoporous Au structures using pump-probe thermoreflectance. Using a modified two temperature model, we determine that the electron Fermi relaxation time is unaffected by the ligament size and is an athermal process that is constant with laser pulse excitation, yet the electron-phonon relaxation is affected by boundary scattering and is dependent on electron temperature. The increased, temperature dependent electron-phonon coupling measurements can be explained by electron-boundary scattering and electron-electron scattering that alters the rate of electron equilibration with the surrounding media. These results lend insight into electron relaxation processes in high surface area nanostructures. © *2011 American Institute of Physics*. [doi:10.1063/1.3530866]

I. INTRODUCTION

Porous materials are of increasing importance in the design and implementation of next generation nanodevices because of their novel mechanical, catalytic, and sensing properties,[1] with recent interest in nanoporous gold (np-Au).[2–6] While nonequilibrium electronic processes in low dimensional structures are becoming critical parameters in nanodevices,[7] these processes are of even more importance in devices with nanoporous structures, since porosities and ligament sizes will volumetrically restrict the electron mean free path. As characteristic lengths decrease in these structures and devices, power densities rise and boundary scattering will dominate electronic relaxation and become a major concern in development and design of future nanoelectronic systems.

In this work, we study the Fermi relaxation time and electron-phonon thermalization time of np-Au structures through pump-probe thermoreflectance. Using a modified two temperature model (TTM), we determine that the electron Fermi relaxation time is unaffected by the ligament size and is an athermal process that is constant with laser pulse excitation, yet the electron-phonon relaxation is affected by boundary scattering and is dependent on electron temperature. Since the nanoporous samples are essentially a random matrix of nanowires, these experimental results provide insight into the Fermi relaxation and electron thermalization processes in metal nanostructures.

II. EXPERIMENTAL CONSIDERATIONS

The amorphous $Au_{35}Si_{65}$ films with a thickness of 600 nm were deposited on HF-cleaned Si substrate using a dual electron beam deposition system. Prior to the Au–Si deposition, a 2 nm Ti layer was deposited to improve the film-substrate adhesion, followed by a 12 nm Au etch-stop layer. Si in the $Au_{35}Si_{65}$ films was electrochemically etched in a 3% HF aqueous solution with an applied potential of 0.8V at room temperature. Four different samples, labeled as np-Au-1 through np-Au-4, all with the same nominal composition were dealloyed leaving nanoporous structures similar to that shown in Fig. 1. The porosity was estimated by measuring the area fraction of the pores from plan view SEM images. The porosities of each of the samples are listed in Table I.

We measure the electron thermalization processes with an ultrafast pump-probe experimental set operating at a repetition rate of 80 MHz, with a 90 fs pulse width, and a central wavelength of 785 nm.[8] The pump pulses are further modulated with an electro-optic modulator (EOM) operating at 11 MHz and the probe pulses are time-delayed using a mechanical delay stage. Due to dispersion introduced by the EOM, the pump pulses are broadened to ~185 fs, as measured via autocorrelation at the sample surface. The coaxial pump and probe pulses are focused onto the sample surface to a spot radius of 15 μm. The reflectance data collected with a photodiode is locked into the pump modulation fre-

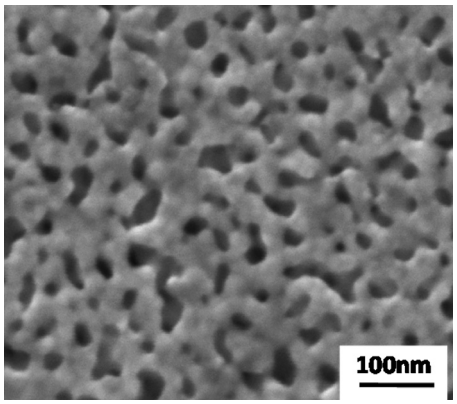

FIG. 1. Scanning electron microscopy micrograph showing the porous morphology of the dealloyed np-Au-1 sample.

a)Electronic mail: pehopki@sandia.gov.

TABLE I. Summary of results from best fit of the thermoreflectance data.

Sample	F (J m^{-2})	G (10^{16} W m^{-3} K^{-1})	Std. dev. (10^{16} W m^{-3} K^{-1})
np-Au-1 porosity 26.70%	3.1	4.1	0.2
	2.0	3.7	0.2
	0.7	2.9	0.2
np-Au-2 porosity 37.30%	3.1	4.5	0.3
	2.0	4.0	0.3
	0.7	3.1	0.2
np-Au-3 porosity 38.50%	3.1	5.0	0.3
	2.0	4.4	0.2
	0.7	3.5	0.2
np-Au-4 porosity 27.30%	3.1	4.0	0.3
	2.0	3.7	0.2
	0.7	3.1	0.3

quency to give the thermoreflectance signal ($\Delta R/R$) as a function of pump-probe delay time. The raw data were adjusted for electronic noise[9] and thermal accumulation from the pump pulses[10] by monitoring the imaginary component of the thermoreflectance response and the pump phase. The temporal thermoreflectance responses of the four np-Au samples are monitored after excitation with three different incident laser fluences, F=3.1, 2.0, and 0.7 J m^{-2}. Figure 2 shows the thermoreflectance data after the 3.1 and 0.7 J m^{-2} pump excitation measured on the np-Au-1 sample along with the data on a 20 nm Au/glass sample, which serves as our calibration. The np-Au film gives a substantially different thermoreflectance signal than the 20 nm Au films for the same incident laser fluence indicating some additional electron scattering mechanism.

The Fermi relaxation time is related to the time it takes for the electron system to reach the peak

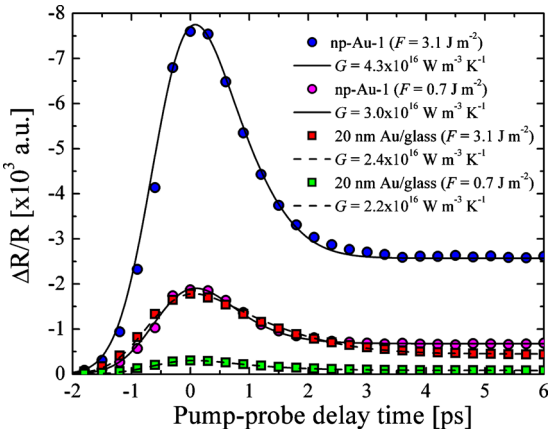

FIG. 2. (Color online) Temporal thermoreflectance data on the np-Au-1 and 20 nm Au/glass samples taken with 3.1 and 0.7 J m^{-2} incident pump fluence. The samples exhibit different thermoreflectance responses at the equivalent incident fluences, indicating different electron scattering mechanisms. The difference in the response of the nanoporous sample is due to electron scattering at the ligament boundaries. The TTM fit to the thermoreflectance data is also presented. G determined on the np-Au structure at the two laser fluences indicates an influence of electron-ligament boundary scattering. This ligament boundary scattering processes is dependent on electron temperature. The value for electron thermalization (Fermi relaxation time) in these Au samples is determined as $t_{th} \approx 1.0 \pm 0.1$ ps for all the samples. Only every third data point is shown for clarity.

thermoreflectances[11,12] and the electron-phonon thermalization time is related to the decay of the thermoreflectance signal after the peak.[13,14] Among these three cases, the Fermi relaxation times are all nearly identical, but the electron-phonon thermalization times are all different. The np-Au sample exhibits a different decay trend compared to the thin film sample, indicating an electron scattering mechanisms in the nanoporous samples that is affecting the electron-phonon thermalization rate in a different manner than the scattering processes in the thin film.

To quantify this, we model the temperature change in the Au films with the standard TTM,[15] only we modify the standard source term to account for a delayed electron thermalization.[16] The traditional source term in the TTM assumes that after pulse absorption, the electron system is fully thermalized. This would mean the peak reflectance would occur ~185 fs after the initial absorption process takes place. As apparent from Fig. 2, this is clearly not the case, as the rise time of the fast transient is ~2 ps. Therefore, we assume the source term in the TTM is given by[16]

$$S(t) = \frac{0.94F(1-R)}{d(t_p + t_{th})} \exp\left\{-2.77\left[\frac{t - 2(t_p + t_{th})}{t_p + t_{th}}\right]^2\right\}, \quad (1)$$

where F is the incident laser fluence, d is the optical penetration depth in Au which at 785 nm is 13.6 nm, R is the surface reflectivity, d is the thermal penetration depth, t_p is the pulse width of the pump pulse at the sample surface (~185 fs), and t_{th} is the delay in the electron thermalization time after pulse absorption. Therefore, the Fermi relaxation time of the electron system can be estimated as $\tau_F = t_p + t_{th}$.

Once the temperature of the electron system is calculated with the TTM, the electron temperature is related to the measured signal through a thermoreflectance model. Since Au has a relatively low electronic heat capacity, the quadratic dependence of the change in reflectance on electron temperature must be accounted for with an interband thermoreflectance model.[17,18] The electron and phonon heat capacities of thin Au films are assumed to be the bulk value.

The reflectivity of the thin Au/glass sample is calculated from thin film optics[19] as back reflections of the laser pulse from the film substrate interface will affect the amount of energy absorbed in the thin film. In the calculations, the components of the indices of refraction for Si and glass are taken from tabulated values.[20] Since the porous material is simply solid ligaments of Au and pockets of nonabsorbing, nonreflecting air, we use a rule of mixing to calculate the reflectivities of the np-Au-1,−2, −3, and −4. The reflectivities are calculated as 70.5%, 62.2%, 61.2%, and 70.0%, respectively. We validate these calculations by examining the reflected probe voltage from the np-Au samples as compared to a bulk, Au sample with ~97% reflectivity at 785 nm. Taking into account the nanoporous medium with air pockets, the effective extinction coefficient—and hence the optical penetration depth—of the medium heated by the pump pulse will also change based on the porosity of the structure. The extinction coefficient, k, of air is k=0, so the optical penetration depths of np-Au-1,−2,−3, and −4 are 18.5 nm, 21.7 nm, 22.1 nm, and 18.7 nm, respectively. For Au, the temperature dependencies of the indices of refraction are calcu-

lated from the Drude-based thermoreflectance model.[17] In the nanoporous samples, we assume that the thermoreflectance response comes solely from the change in temperature of the solid Au ligaments, since the air pockets in the nanoporous structure are nonabsorbing. Therefore, the thermoreflectance response is dictated by the intraband reflectance model[17] with no further modification needed for the porosity since reflectivity due to the increased porosity is accounted for in the source absorption term of the TTM (and, therefore, the increased temperature rise is accounted for in the np-Au samples).

The TTM fit to the data presented in Fig. 2. The best fit G on the 20 nm Au/glass film agrees well with previously determine electron-phonon coupling factor measurements on bulk and thin film Au at low fluence.[18,21,22] The best fit G on the np-Au-1 data shows an increase from G measured on the 20 nm thin film sample when subjected to the 3.1 J m^{-2} incident fluence excitation. The increase in G is also apparent in the low fluence data on the np-Au-1 samples. The nanoporous films are ~300 nm thick, such that it can be considered semi-infinite since the thermal penetration depth of the nonequilibrium electrons is ~100 nm,[14] indicating that electron-interface scattering at the np-Au/substrate interface is negligible in the np-Au samples. This increase could, therefore, be due to electron-boundary scattering at the ligament boundaries in the nanoporous samples. In addition, since the enhancement in the electron-phonon coupling factor decreases with decreasing incident fluence (i.e., a decrease in electron temperature), this indicates that electron-boundary scattering affects the electron scattering processes in a thermal fashion, unlike the typically assumed boundary scattering processes in nanostructures, which takes the temperature independent form of $\tau_b = D/v$, where D is the characteristic length of the structure and v is the carrier velocity. In all the samples, the delay in electron thermalization is relatively constant and independent of laser fluence. The value for electron thermalization (Fermi relaxation time) in these Au samples is determined as $t_{th} \approx 1.0 \pm 0.1$ ps. This delayed thermalization is consistent with previously determined values in Au.[16,23] This is also consistent with Fermi liquid theory, which states that single particle lifetime above the Fermi level is related to the energy above the Fermi level [$t_{th} \propto (E-E_F)^{-2}$ where E is the electron energy and E_F is the Fermi energy].

III. DISCUSSION

A summary of the best fit values for G of each sample at the three incident laser fluences is presented in Table I. We observe a dependency on boundary scattering in all the nanoporous Au samples, with a further temperature dependency of this boundary scattering. This is apparent in Fig. 3, which graphs the best fit G from the np-Au samples as a function of maximum electron temperature after pulse absorption. We estimate the maximum electron temperature by[14] $T_{e,\max} = \sqrt{2(1-R)F/(d\gamma)}$, where γ is the linear coefficient to the electron heat capacity, which for Au is 62.9 J m^{-3} K^{-2}.[24] Although a less drastic temperature dependency was observed in thin film samples at near IR wavelengths,[21,22] this temperature dependency is due to a different interaction mechanism. In thin film samples, electron-interface scattering at the film/substrate interface can cause phonon emission into the substrate, thereby increasing the rate of electron-phonon interaction.[21,25,26] However, electron scattering at the isolated boundaries in the nanoporous sample would not emit phonons into the adjacent materials, since the boundary of the ligament is adjacent to air. This parallels the electron-boundary scattering mechanism in an isolated/suspended nanowire.

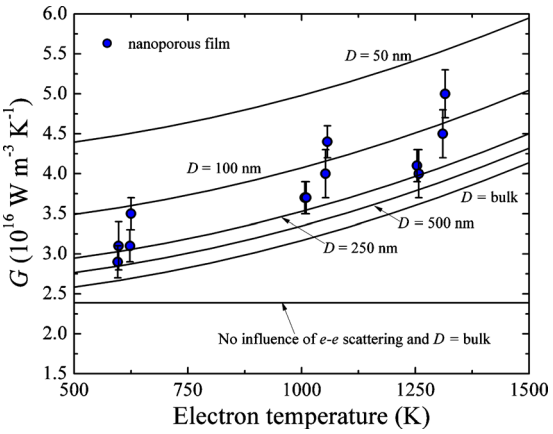

FIG. 3. (Color online) Electron–phonon coupling factors as a function of electron temperature for the np-Au samples and calculations of Eq. (4) using the average electron-boundary scattering time for 4 different values of $D_{\max}$ and assuming a phonon temperature at 300 K. The calculations of Eq. (4) agree well with the nanoporous Au measurements, indicating that in nanoporous metals, increased electron-electron and electron-boundary scattering mechanisms are affecting the overall rate of electron-phonon heat transfer. The temperature dependency can be explained by accounting for electron-electron interaction and an additional temperature independent increase ascribed to electron-boundary scattering.

In metals with temperatures above the Debye temperature, electron-phonon scattering is given by[27]

$$G = \frac{9nk_B^2\theta_D^2}{16T_pE_F\tau_{ep}(T_p)}, \tag{2}$$

where n is the electron number density, k_B is the Boltzmann constant, θ_D is the Debye temperature, T_p is the phonon temperature, and τ_{ep} is the electron-phonon scattering time. The electron-phonon scattering time is proportional to the phonon temperature, T_p ($\tau_{ep}^{-1} = B_{ep}T_p$, where B_{ep} is the electron-phonon interaction constant), leading to the temperature independent electron-phonon coupling factor in bulk materials, as indicated by the horizontal line in Fig. 3. In thin films, a high electron temperature means that the electrons and phonons will stay out of equilibrium in the film for a longer time assuming a constant electron-phonon coupling factor. This leads to more electrons reaching the film/substrate interface without losing energy to the film phonons, thereby, increasing the phonon emission into the substrate via film electron scattering at the film/substrate interface. In nanoporous materials, high energy electrons that reach the ligament boundaries before losing energy to phonons in the ligaments do not emit phonons into the adjacent air, as previously discussed. However, after scattering at the ligament boundaries, the redirected electrons will be more likely

to interact with other electrons before completely thermalizing with the phonon system, thereby causing electron-electron scattering to play a greater role in high surface area nanostructures than in bulk materials. Since the measured thermoreflectance decay is related to all the electron relaxation mechanisms, we recast Eq. (2) to account for electron-electron and electron-boundary scattering which could affect the relaxation that is measured in the data. We define a total electron relaxation rate as during electron-phonon nonequilibrium as

$$G^* = \frac{9nk_B^2\theta_D^2}{16T_pE_F\tau_t(T_e,T_p)}, \tag{3}$$

where τ_t is the total electron scattering time and accounts for electron-electron, electron-phonon, and electron-boundary scattering. Through Matthiessen's rule, this scattering time is given by

$$\tau_t^{-1} = A_{ee}T_e^2 + B_{ep}T_p + \frac{v_F}{D}, \tag{4}$$

where A_{ee} is the electron-electron scattering constant, which can be deduced from low temperature electrical resistivity measurements in bulk materials where electron-electron scattering dominates,[24] T_e is the electron temperature, and v_F is the Fermi velocity. In Au, $A_{ee}=1.2\times10^7$ K^{-2} s^{-1} and $B_{ep}=1.23\times10^{11}$ K^{-1} s^{-1} and are constant with temperature,[28–31] and v_F is 1.4×10^6 m s^{-1}.[24] Equation (4) together with Eq. (3) describes the total electronic relaxation measured in the TTR data. The calculations of Eq. (3) using only literature values for the thermophysical properties of Au agree well with the nanoporous Au measurements, indicating that in nanoporous metals, increased electron-electron and electron-boundary scattering mechanisms are affecting the electronic thermal relaxation.

The idea that various electronic relaxation mechanisms, such as electron-electron and electron-boundary scattering, affect the overall rate of electron-phonon coupling is consistent with Kaganov *et al.*'s original theory on electron-phonon coupling.[32,33] The general conceptual idea behind this is that electron-phonon coupling is related to the electronic temperature and energy. This is clear from the electron-electron scattering time which is proportional to T_e^2. Although the electron-boundary scattering rate does not affect the overall electron temperature or energy, the electron-boundary interaction leads to an increase in phonon emission; this parallels the idea of electron-surface phonon interactions assuming the surface phonons are described by portions of the bulk phonon spectrum. Note that all of these processes also affect the transient thermoreflectance response.[17,34] Another electronic scattering mechanism that is not considered in this analysis is electron-defect scattering. However, it was previously shown that for Au nanosystems of similar characteristic dimensions as the np-samples in this study, when electrons are out of equilibrium with the phonons, electron-boundary scattering far out-weighs electron-defect scattering.[17]

IV. SUMMARY

In summary, we investigate electron-phonon heat transfer in nanoporous metals. We use a pump-probe thermoreflectance technique to measure the electron-phonon coupling factor in np-Au films. The measured electron phonon coupling factor is higher than the bulk value for Au, and shows a dependency with electron temperature. The increased, temperature-dependent electron-phonon coupling factor can be explained by electron-boundary scattering and electron-electron scattering that is altering the electron-phonon interaction. Similar phenomena are expected in electron-phonon heat transfer in nanowires and other high surface area nanostructures.

ACKNOWLEDGMENTS

P.E.H. is greatly appreciative for funding from the LDRD program office through Sandia National Laboratories. The authors would like to thank Dr. S. T. Picraux at Los Alamos National Laboratories for insightful discussions. This work was performed, in part, at the Center for Integrated Nanotechnologies, a U.S. Department of Energy, Office of Basic Energy Sciences user facility; the authors would like to thank John Sullivan for assistance regarding work at the Center for Integrated Nanotechnologies. Sandia is a multiprogram laboratory operated by Sandia Corporation, a Lockheed-Martin Co., for the United States Department of Energy's National Nuclear Security Administration under Contract No. DE-AC04-94AL85000.

[1] S. Polarz and B. Smarsly, J. Nanosci. Nanotechnol. **2**, 581 (2002).
[2] J. Biener, A. M. Hodge, J. R. Hayes, C. A. Volkert, L. A. Zepeda-Ruiz, A. V. Hamza, and F. F. Abraham, Nano Lett. **6**, 2379 (2006).
[3] J. S. Biteen, D. Pacifici, N. S. Lewis, and H. A. Atwater, Nano Lett. **5**, 1768 (2005).
[4] H.-M. Bok, K. L. Shuford, S. Kim, S. K. Kim, and S. Park, Nano Lett. **8**, 2265 (2008).
[5] P. E. Hopkins, P. M. Norris, L. M. Phinney, S. A. Policastro, and R. G. Kelly, J. Nanomater. **2008**, 418050 (2008).
[6] Z. Liu and P. C. Searson, J. Phys. Chem. B **110**, 4318 (2006).
[7] A. Majumdar, K. Fushinobu, and K. Hijikata, J. Appl. Phys. **77**, 6686 (1995).
[8] P. E. Hopkins, J. R. Serrano, L. M. Phinney, S. P. Kearney, T. W. Grasser, and C. T. Harris, J. Heat Transfer **132**, 081302 (2010).
[9] A. J. Schmidt, R. Cheaito, and M. Chiesa, Rev. Sci. Instrum. **80**, 094901 (2009).
[10] R. J. Stevens, A. N. Smith, and P. M. Norris, Rev. Sci. Instrum. **77**, 084901 (2006).
[11] C. K. Sun, F. Vallee, L. H. Acioli, E. P. Ippen, and J. G. Fujimoto, Phys. Rev. B **48**, 12365 (1993).
[12] C. K. Sun, F. Vallee, L. H. Acioli, E. P. Ippen, and J. G. Fujimoto, Phys. Rev. B **50**, 15337 (1994).
[13] S. D. Brorson, A. Kazeroonian, J. S. Moodera, D. W. Face, T. K. Cheng, E. P. Ippen, M. S. Dresselhaus, and G. Dresselhaus, Phys. Rev. Lett. **64**, 2172 (1990).
[14] J. Hohlfeld, S. S. Wellershoff, J. Gudde, U. Conrad, V. Jahnke, and E. Matthias, Chem. Phys. **251**, 237 (2000).
[15] S. I. Anisimov, B. L. Kapeliovich, and T. L. Perel'man, Sov. Phys. JETP **39**, 375 (1974).
[16] P. E. Hopkins, L. M. Phinney, and J. R. Serrano, "Reexamining electron-Fermi relaxation in gold films with a nonlinear thermoreflectance model," J. Heat Transfer (2011) (unpublished).
[17] P. E. Hopkins, J. Appl. Phys. **105**, 093517 (2009).
[18] A. N. Smith and P. M. Norris, Appl. Phys. Lett. **78**, 1240 (2001).
[19] F. Abeles, in *Advanced Optical Techniques*, edited by A. C. S. V. Heel (North-Holland, Amsterdam, 1967), p. 145.

[20]E. D. Palik, *Handbook of Optical Constants of Solids* (Academic, Orlando, 1985).
[21]P. E. Hopkins, J. L. Kassebaum, and P. M. Norris, J. Appl. Phys. **105**, 023710 (2009).
[22]P. E. Hopkins and P. M. Norris, Appl. Surf. Sci. **253**, 6289 (2007).
[23]W. S. Fann, R. Storz, H. W. K. Tom, and J. Bokor, Phys. Rev. B **46**, 13592 (1992).
[24]C. Kittel, *Introduction to Solid State Physics*, 7th ed. (John Wiley, New York, 1996).
[25]M. L. Huberman and A. W. Overhauser, Phys. Rev. B **50**, 2865 (1994).
[26]A. V. Sergeev, Phys. Rev. B **58**, R10199 (1998).
[27]T. Q. Qiu and C. L. Tien, J. Heat Transfer **115**, 842 (1993).
[28]D. E. Gray, *American Institute of Physics Handbook*, 3rd ed. (McGraw-Hill, New York, 1972).
[29]M. Kaveh and N. Wiser, Adv. Phys. **33**, 257 (1984).
[30]A. H. MacDonald, Phys. Rev. Lett. **44**, 489 (1980).
[31]X. Y. Wang, D. M. Riffe, Y.-S. Lee, and M. C. Downer, Phys. Rev. B **50**, 8016 (1994).
[32]M. I. Kaganov, I. M. Lifshitz, and L. V. Tanatarov, Sov. Phys. JETP **4**, 173 (1957).
[33]J. K. Chen, W. P. Latham, and J. E. Beraun, J. Laser Appl. **17**, 63 (2005).
[34]P. E. Hopkins, Phys. Rev. B **81**, 035413 (2010).